Available online at www.sciencedirect.com
ScienceDirect
Applied Surface Science 253 (2007) 5173–5178
applied surface science
www.elsevier.com/locate/apsusc

Biosensing of biophysical characterization by metal-aluminum nitride-metal capacitor

Chang-Chih Chen [a,b], Che-Tong Lin [a,c], Sheng-Yang Lee [a,d], Ling-Hung Lin [a,c], Chiung-Fang Huang [a,c], Keng-Liang Ou [e,f,*]

[a] School of Dentistry, College of Oral Medicine, Taipei Medical University, Taipei 110, Taiwan
[b] Department of Emergency Medicine, Mackay Memorial Hospital, Taipei 104, Taiwan
[c] Department of Dentistry, Taipei Medical Hospital, Taipei Medical University, Taipei 110, Taiwan
[d] Department of Dentistry, Wan-Fang Hospital, Taipei Medical University, Taipei 110, Taiwan
[e] Graduate Institute of Oral Sciences, College of Oral Medicine, Taipei Medical University, Taipei 110, Taiwan
[f] Graduate Institute of Biomedical Materials and Engineering, College of Oral Medicine, Taipei Medical University, Taipei 110, Taiwan

Received 20 September 2006; received in revised form 18 November 2006; accepted 20 November 2006
Available online 27 December 2006

Abstract

Aluminum nitride thin films were fabricated as stress biosensors for biosensing cell attachment. The features and capacitance of AlN films following cell culture were detected via leakage current density and biocompatibility testing. Analytical results demonstrate that the failure of the capacitors produced slit-like microvoids to form on the AlN film, following cell differentiation and proliferation. Slit-like microvoids incurred substantial current leaking of the cell cultured-capacitor, even at a low breakdown voltage. Stress variation during cell differentiation and proliferation were responsible for the formation of microvoids and the low breakdown voltage. The stress produced lattice distortion of the AlN film, resulting in a piezoelectric effect on the AlN film surface. Results of this study demonstrate that the piezoelectric AlN film is highly promising as a biosensing film.

Keywords: Aluminum nitride; Thin film; Biocompatibility; Differentiation; Proliferation

1. Introduction

Titanium and its alloys (Ti-6Al-4V) are extensively adopted as common materials for bone implants [1–8]. Interactions between cell behavior and the implant are critical to tissue healing. Moreover, interactions between cell behaviors, including cell proliferation and cell differentiation, and the implant also directly affect the healing time [5,8]. Various procedures have been employed to modify implant surfaces to promote bone-tissue integration [8–16]. Of these numerous techniques, surface coating effectively improves cell attachment, cell proliferation and cell differentiation. Topographic features on the implants range from millimeters to nanometers and are all believed to enhance the biological response of the host [11]. The improvement of cell attachment is important in reducing the healing time during which, the patient has an embedded implant [14,18]. Accordingly, observing and evaluating the true healing situation are also important. Fabricating bioactive implant surfaces and monitoring cell attachment are important when working with medical implants, including dental implants, mini-implants and bone plates. In this investigation, a new biosensing method is presented to detect the attachment of cells to the implant with a piezoelectric thin film coating. Aluminum nitride was deposited on implants as a biosensing thin film. The stress was measured to elucidate the reaction of bone cells to the AlN film. The characteristics of Al-N thin films with and without a cell culture were measured electrically and by material analyses. A cell culture was also applied to investigate the biocompatibility of an Al-N film.

* Corresponding author at: Graduate Institute of Oral Sciences, College of Oral Medicine, Taipei Medical University, Taipei 110, Taiwan.
Tel.: +886 2 27361661x5400; fax: +886 2 27362295.
E-mail address: klou@tmu.edu.tw (K.-L. Ou).

0169-4332/$ – see front matter
doi:10.1016/j.apsusc.2006.11.037

2. Materials and methods

2.1. Preparation of titanium substrate

An ASTM F67 Grade II Ti sheet, with a thickness of 1 mm, was used as received as the substrate. It was cut into discs with a diameter of 14.5 mm for use in experiments. All specimens were mechanically polished using 1500 grit paper and were further polished using diamond abrasives. The specimens were finished by applying colloidal silica abrasives. Before use, all sheets were degreased and pre-pickling in acid by washing in acetone, and processing them through 2% ammonium fluoride, a solution of 2% hydrofluoric acid and 10% nitric acid at room temperature for 60 s. Finally, the specimens were etched in an aqueous mixture of HF (2 vol%) and HNO_3 (4 vol%) at room temperature for numerous seconds, and then washed in distilled water in an ultrasonic cleaner.

2.2. Preparation of metal-aluminum nitride-metal capacitor

An Si(1 0 0) wafer with a resistivity 6–9 Ωcm was utilized as a substrate to deposit an Al-N film by RF magnetron sputtering. The target of the sputtering was a 4 in. piece of 99.999% aluminum. The key feature of this experiment was the use of various nitrogen flow rates during the sputtering of Al-N films. On top of the Si substrate, 1000 nm-thick thermal oxides were grown as buffers, on which copper was deposited. A Ta (10 nm-thick) layer was deposited on Cu by sputtering and Al-N films were then subsequently deposited by magnetron reactive sputtering using an Al target. The plasma power was 20 W/cm^2 in N_2/Ar, as the substrate temperature was increased from room temperature to 400 °C. Before the Cu top electrodes were deposited, the NIH3T3 cell (fibroblast cell lines) was cultured on AlN/Ta/Cu systems for 4, 8 h, 1, 2, 3, 5 and 7 days. The top electrodes of Cu (350 nm) were finally deposited by sputtering to make electrical current–voltage (*I–V*) measurements.

2.3. Evaluations of bone cells on AlN film

Cell proliferation on titanium and surface-modified Ti plates was examined in each test, and that on 24-well polystyrene plates was studied as controls. Titanium plates under various conditions were placed into the 24-well polystyrene plates, and an NIH3T3 cell suspension was placed on the plate with a density of 5×10^4/cm^2. Plastic culture plates were applied as a positive control. After cell culture for 1, 4, 8 h, 1, 2, 3, 5 and 7 days, the cells that did not attach were washed away using PBS (0.1 M, pH 7.2). Into every culture plate, 500 μl culture solution and 50 μl 3-(4,5-dimethylthiazol-2-yl)-2,5-diphenyl-tetrazolium bromide (MTT) label solution were added, and the plates were placed into a culture chamber at 37 °C with under 5% CO_2. Active cells produced formazan salt for 4 h, and then the buffer solution (10% SDS/0.01 M HCl, 500 μl/well) was added. Overnight, light with a wavelength of 595 nm was used to determine the cell optical density (OD). Each group used for cell culture comprised 50 samples. The above procedure was conducted five times as to obtain an average value, which was compared with the value from the controls. Finally, cell attachment and proliferation were observed) by scanning electron microscopy (SEM).

2.4. Properties of capacitors with and without cell attachment

MIM capacitors (Cu/AlN/Ta/Cu/SiO_2 and Cu/cell/AlN/Ta/Cu/SiO_2) were electrically analyzed to investigate cell reactions with the capacitance of Al-N films. The leakage current of a structure was measured using an HP4145B semiconductor parameter-analyzer. The interface microstructure was examined by transmission electron microscopy (TEM). Cross-sectional TEM samples were prepared to be transparent to electrons using a focused ion beam (FIB).

2.5. Statistical analysis

The *t*-test was conducted to the significance of the observed differences between the percentage of attached cells on the Ti and that on surface-modified Ti. Each statistical test has an associated null hypothesis, and the *p*-value is the probability that the sample could have been drawn from the tested population(s). A *p*-value of 0.05 indicates that the probability of drawing the tested sample, if the null hypothesis is true, is 5%.

3. Results and discussion

Fig. 1 shows a series of glancing-angle X-ray diffraction patterns of Al-N films deposited on Ti substrates at various nitrogen flow ratios (*f*). The (1 1 1) peak confirms that the aluminum nitride film on Ti has a face-centered cubic structure (fcc-Al(N)). The microstructural variation of Al and Al-N films is from fcc-Al to fcc-Al(N) as the nitrogen flow ratio increases. The phase transition from fcc-Al(N) to bcc-Al(N) was also observed as the nitrogen flow ratio was increased to 50%. When the nitrogen flow ratio was increased to 70%, the relatively (0 0 2)-preferred orientation of the hcp-AlN was examined. The GIXRD results clearly reveal that microstructural variation proceeds as fcc-Al(N) → bcc-Al(N) → hcp-AlN phases suc-

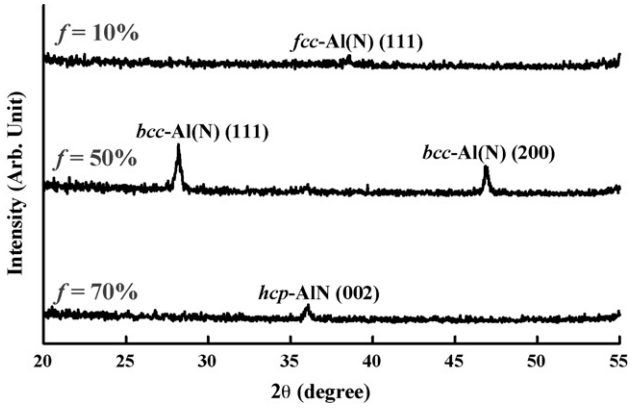

Fig. 1. GIXRD of Al-N films following various nitrogen flow ratio.

cessively as the nitrogen flow ratio is increased from 10 to 70%. Fig. 2 presents images of various Al-N films on Ti substrates obtained by atomic force microscopy (AFM). In Fig. 2(a), an AFM image of the α-Al(N) film shows grains with a pentagonal morphology and a low surface roughness of 21.3 ± 4 nm RMS. TEM analyses demonstrated that the crystallographic microstructure of α-Al(N) is face-centered cubic (fcc) structure. The fcc-AlN film yielded similar results, indicating that the surface roughness approaches 28.2 ± 2 nm. Additionally, as the nitrogen flow ratio is increased to 70%, the crystallographic structure transformed to hcp-AlN, as determined by GIXRD. The AFM image shows larger grains than those of α-Al(N) or fcc-AlN, associated with increased surface roughness (RMS = 48.12 ± 6 nm), as presented in Fig. 2(b). The GIXRD and AFM results reveal a microstructural variation from fcc polycrystalline Al to fcc-Al(N). For a nitrogen flow ratio below a critical value, this microstructural variation yields a metastable polycrystalline fcc polycrystalline microstructure. As the nitrogen flow ratio is increased above the threshold value, a transition from metal-sputtering to nitride sputtering was observed, substantially increasing the nitrogen concentration and promoting the formation of polycrystalline with large grains and a rough nitride film. Analysis of the TEM micrograph and the selected area diffraction pattern of a nitrogen-incorporating AlN film demonstrated a (0 0 2) diffraction ring pattern, which confirms that the AlN film on the Ti substrate has a hexagonal close packed structure. The micrograph clearly indicates that the individual columnar grains are closely packed and large. Additionally, numerous sharp rings were observed in the diffraction pattern of the as-sputtered hcp-AlN film, indicating that the as-sputtered AlN film had a nano/polycrystalline structure. Ou observed similar results [17]. As stated above, the release of metallic ions results in poor osseointegration and often causes clinical failure [18]. Although the release of metallic ions may be harmful, metal-based implants have been adopted extensively because of their great strength [19]. Hence, their corrosion resistance and bioactive characteristics can be improved. Metal nitride films can induce and nucleate apatite [20]. Furthermore, the topographic characteristics of the implants, ranging from millimeters to nanometers, are believed to influence the biological response of the host [11].

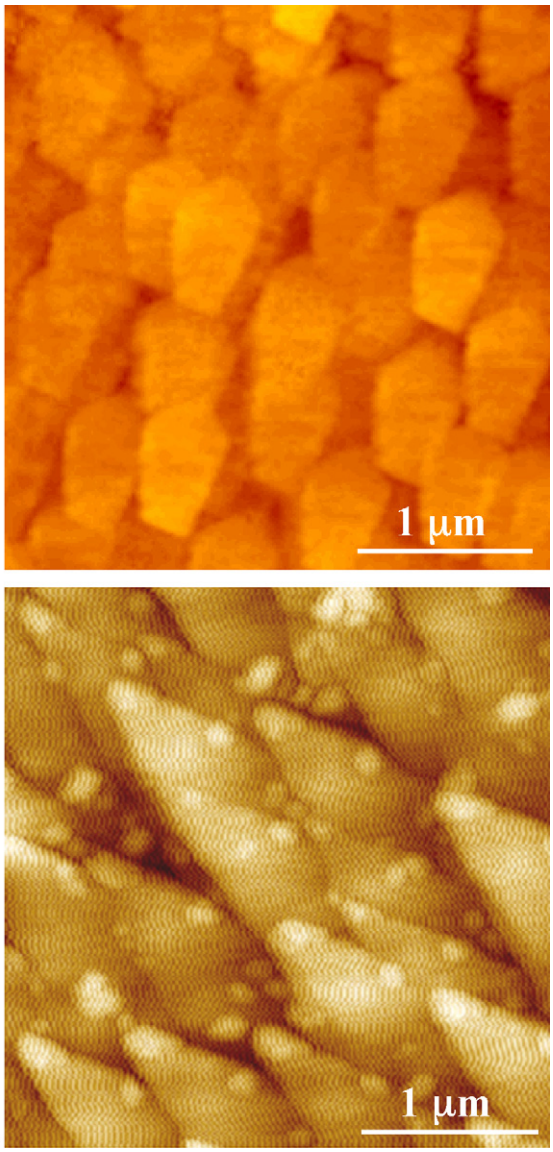

Fig. 2. AFM images of Al-N films deposited on Ti under various nitrogen flow ratio: (a) 30%, and (b) 70%.

The electrical resistivity of Al-N film in relation to the nitrogen flow ratio was also measured using a four-probe system. The resistivity of the as-deposited film has numerous interesting characteristics. The electrical resistivity of the Al film is 2.9 ∼ 3.21 μΩcm. The resistivity increases slightly when a small amount of nitrogen is added to the sputtering gas. The resistivity of the film increases to 33.41 μΩcm when the nitrogen flow ratio is 10%. As more nitrogen is incorporated into the Al film, the resistivity of the $AlN_{0.44}$ film rises to 45000 ∼ 47000 μΩcm and that of the $AlN_{0.53}$ film increases to 54000 ∼ 56000 μΩcm. Moreover, the microstructure and phase transformations vary the resistivity. The labels β-Al(N), α-Al(N), fcc-AlN and hcp-AlN in the GIXRD patterns indicate a series of microstructural variations. Theoretical studies of piezoelectric films have demonstrated that aluminum nitride (AlN) provides advantages over ZnO, such as an excellent acoustic velocity and high resistivity [21]. The deposited-AlN was grown in a hexagonal B4 wurtzite structure with high resistivity and a direct optical band gap. Therefore, AlN is believed to inhibit photo scattering, and increase ballistic electron velocities when a biosensing device is applied.

Cells spread effectively on titanium with an hcp-AlN coating after various culture times, suggesting good attachment, as displayed in Fig. 3, in which the cell morphology is heterogeneous. The cells fully adapted to the AlN/Ti and Ti. After 8 h of cell culture, SEM examination demonstrated that the cells on Ti and AlN/Ti were round with central, protruding nuclei that were surrounded by a thin rim of cytoplasm (Fig. 3(a and b)). Fig. 3(c and d) display cell surface morphology on Ti and AlN/Ti after culturing for 24 h, respectively. Protruding nuclei can still be observed on the cells on the Ti surfaces, even though some cells were flat, well spread and polygonal.

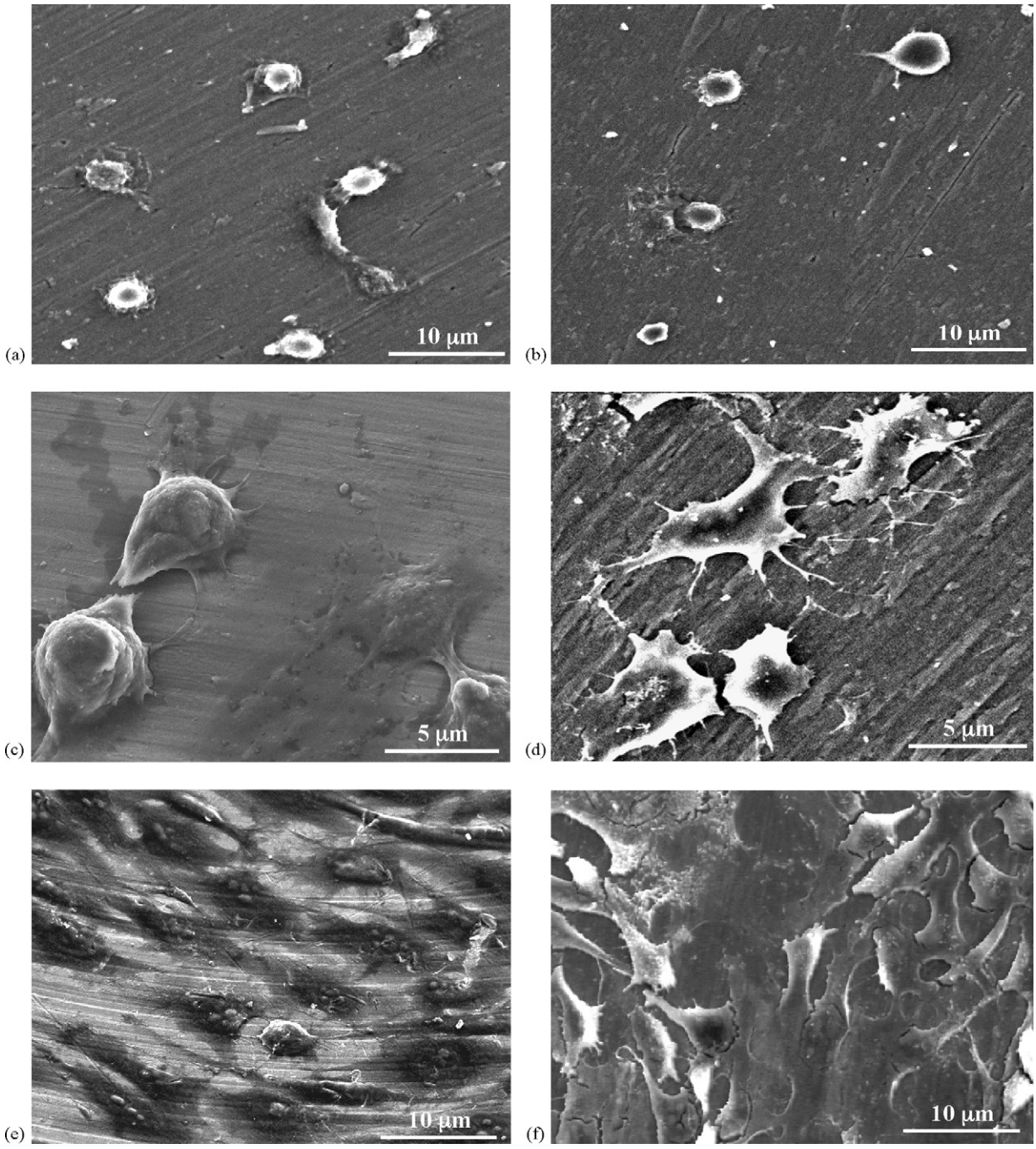

Fig. 3. SEM micrographs demonstrating cellular morphology of Ti and AlN/Ti after various culture times: (a and b) 8 h, (c and d) 24 h, and (e and f) 48 h.

Additionally, the cells on the AlN/Ti surfaces have no clear orientation. The cells were flat, well spread and clearly polygonal without protruding nuclei. After culturing for 24 h, the cells were more elongated than after culturing for 12 h. After 48 h of culturing on Ti, as displayed in Fig. 3(e), most of the cells had begun to grow along the machined tracks and fine irregularities. Moreover, most had begun to differentiate along the fine irregularities after 48 h of culture, as displayed in Fig. 3(f), and the cultured cells were strongly attached, elongated, flat and irregularly networked, indicating that the AlN/Ti had greater biocompatibility than Ti. On the AlN/Ti, the cells were mostly polygonal, flat and well spread, without a particular orientation.

Table 1 presents the cell counting results for Ti and AlN/Ti. The first reactions following seeding included anchorage, attachment, adhesion, migration and cell division. After 8 h of culture, the cells were attached and adherent, but not significantly spread. The attachment of fibroblast cell lines exhibited only minor variation. After 12 h of culture, the cells had spread to virtually all of the surfaces of interest. More cells were attached to the AlN/Ti than to the Ti. The attachment assay with 24 h culture indicated that significantly ($p < 0.05$)

Table 1
Cell counting results for Ti and AlN/Ti

Time (h)	Ti (cells/0.79 cm^2)	AlN/Ti (cells/0.79 cm^2)
8	104 ± 3.3	113 ± 5.3
12	217 ± 5.5	304 ± 7.8
24	335 ± 8.3	587 ± 8.5
48	612 ± 8.4	1045 ± 6.5

more cells were attached to the AlN/Ti than to the Ti. After 48 h of culture, more cells had attached to AlN/Ti surfaces. The number of cells on AlN/Ti was double that on Ti. The percentage of cells attached considerably exceeded that on the Ti specimens. Based on these results, the growth rate of cells on AlN/Ti exceeded that on Ti. The results of the MTT assay with serial dilutions of the extracts of the AlN/Ti implant on 3T3 cells were also studied. The MTT assay revealed that significantly ($p < 0.05$) more cells attached to the AlN/Ti. A difference in biocompatibility with osteoblasts between surface-treated and non-treated titanium is noted. The implants probably require careful and controlled modification of their surface properties [22]. Titanium-based implants are well known to be highly biocompatible. After the surfaces of titanium-based implants have been modified, the implants exhibit better functionality and biocompatibility [22]. Variations in surface properties caused by surface modifications are believed to be important in increasing biocompatibility.

The stress-biosensing capability of thin AlN films with and without cell culturing was further examined by evaluating the stress stability of Cu/biosensing film/Cu MIM capacitor using electrical measurements. Fig. 4 plots the statistical distributions of reverse bias leakage current density for a biosensing film MIM capacitor cultured for 5 days. If a failure threshold is defined as 10^{-5} A/cm^2, then the Cu/AlN/Ta/Cu remained stable after culturing for 5 days. Fig. 4 also plots the statistical distribution of a leakage current density for the Cu/cell/AlN/Ta/Cu cultured for 5 days. The capacitor with a 50 nm-thick AlN film did not maintain a low leakage current density after culturing. After 5 days of culturing, the capacitor failed. Cell reaction and cell attachment on AlN film can be detected using

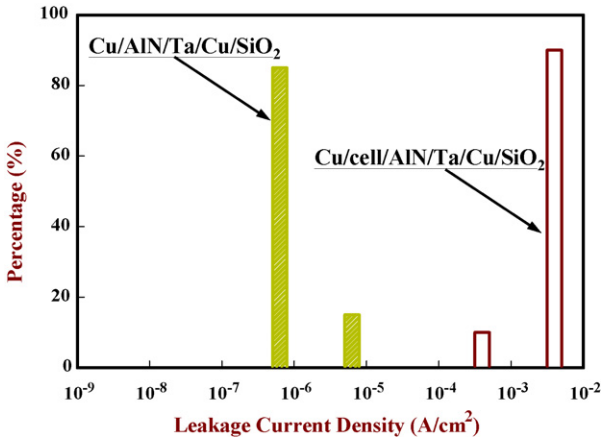

Fig. 4. Histograms of the distributions of leakage current densities for AlN MIM capacitors with and without cell cultures.

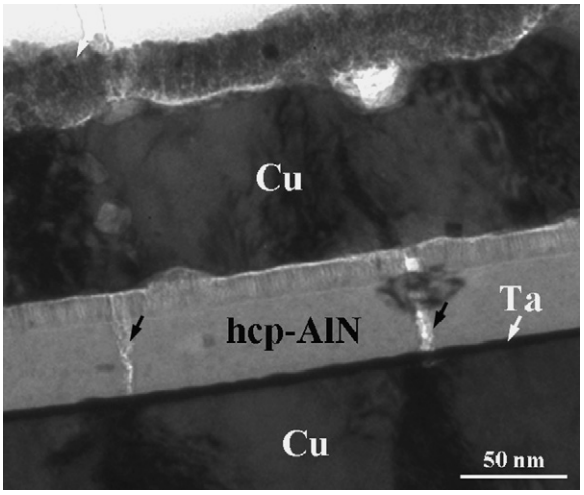

Fig. 5. The cross-sectional TEM micrograph of AlN MIM capacitor with cell.

a Cu/biosensing film/Cu MIM capacitor. In this measurement, the leakage current densities were determined as averages over 30 samples, and the detection areas were 300 μm × 300 μm and 500 μm × 500 μm, respectively. AlN with cells exhibited serious leakage. No such leakage was evident in the AlN specimen without cells, as displayed in Fig. 4. In particular, the current–voltage curve of the cell/AlN specimen was steep, indicating that most of the current had passed through the dielectric layer even before the capacitor was broken down. Fig. 5 presents the cross-sectional microstructure of AlN with NIH3T3 cells. No hillock appeared along any interface between the AlN or Cu electrode in the specimens. This fact revealing that the Ta interlayer was effective in releasing initial stress during sputtering. Additionally, the failure of the AlN MIM capacitor was demonstrated to be possible, even when the interfacial reaction between the dielectric and the metal electrode is substantially suppressed. Slit-like microvoids (indicated by arrows) were observed across the cell/AlN film, but not in the AlN specimen without a cell. This result demonstrates that the failure was not electrical but mechanical. A microvoid is likely to constitute an electrical path, eventually breaking down the capacitor at a low applied voltage. The microvoids herein were caused by a stress variation in a constituent layer of the AlN MIM capacitor. The stress of the thin film after cell culturing comprises the stress (σ_{cell}) induced by the cell reaction and the intrinsic stress (σ_i); the latter is negligible. The total stress of each layer of the specimens was determined by considering only the two adjacent layers as a thin film and a substrate, respectively. The results of the calculation established that the stress variation before and after cell interaction changed from compressive (−1.6 GPa) to tensile (+0.9 GPa) and vice versa, across the boundary of the AlN film and the bone cell layer. According to the analysis of stress variation, the stress flow that accompanied thin film defects, such as voids, dislocation and slips, occurred when the bone cell reacted with the thin film. The stress caused by bone cells seems to be large enough to cause mechanical failure in the MIM capacitor with microvoids, as observed in all specimens. An osseointegrated

implant is physiologically equivalent to an ankylosed bone or tooth, because of its osseous attachment. A high-quality implant should provide an excellent surface that promotes rapid bone healing. Since a bone cell can undergo internal expansion or contraction, changes in osseous structure proceed via cell-mediated resorption and formation. Hence, healing between the bone and the implant is related to biomechanical factors, including surface strain [23]. The internal turnover of osseous tissue is called remolding. Remolding is controlled by both metabolic and biomechanical mechanisms [24], and is important to the postoperative healing of cortical bone [25].

4. Conclusion

This investigation evaluated the biosensing ability of AlN films using cell/AlN MIM capacitors. AlN with a (0 0 2)-preferred orientation was reported to exhibit strong piezoelectricity. The biosensing capability of the bone cell/AlN MIM capacitors was proportional to the strength of cell attachment to the AlN film. Variation in stress associated with cell differentiation and proliferation caused the formation of microvoids. The *cells-induced* stress resulted in lattice and/or atomic displacement and distortion of the AlN film. The AlN film was responsible for a piezoelectric effect on the surface during bone healing. An electromagnetic device can be employed to detect and monitor the piezoelectric effect on an AlN/implant in situ. Even though the detection of a piezoelectrical signal, caused by cell attachment on an implant with an AlN coating, may be limited, the AlN film performs effectively in biosensing and biophysical detection, and thus has potential for use in wireless technology for monitoring cell attachment in situ.

Acknowledgments

The work was financially supported by the National Science Council of the Republic of China under Contract No. NSC94-2320-B-038-014. The authors thank graduate Po-Te Lee for his assiatance.

References

[1] B. Feng, J.Y. Chen, S.K. Qi, L. He, J.Z. Zhao, X.D. Zhang, J. Mater. Sci. Mater. Med. 13 (2002) 457.
[2] M. Takemoto, S. Fujibayashi, M. Neo, J. Suzuki, T. Kokubo, T. Nakamura, Biomater 26 (2005) 6014.
[3] H.H. Kim, F. Miyaji, T. Kokubo, S. Nishiguchi, T. Nakamura, J. Biomed. Mater. Res. 5 (1999) 100.
[4] H.B. Wen, Q. Liu, J.R. De Wijn, K. De Groot, F.Z. Cui, J. Mater. Sci. Mater. Med. 9 (1998) 121.
[5] H.C. Cheng, S.Y. Lee, C.M. Tsai, C.C. Chen, K.L. Ou, Electrochem. Solid-State Lett. 9 (2006) D25.
[6] S. Fujibayashi, T. Nakamura, S. Nishiguchi, J. Tamura, M. Uchida, H.M. Kim, T. Kokubo, J. Biomed. Mater. Res. 56 (2001) 562.
[7] J.R. Goldberg, J.L. Gilbert, Biomater 25 (2004) 851.
[8] Y.M. Yeh, C.S. Chen, M.H. Tsai, Y.C. Shyng, S.Y. Lee, K.L. Ou, J. J. Appl. Phy. 44 (2) (2005) 1086.
[9] H.M. Kim, T. Kokubo, S. Fujibayashi, S. Nishiguchi, T. Nakamura, J. Biomed. Mater. Res. 52 (2000) 553.
[10] X.X. Wang, S. Hayakawa, K. Tsuru, A. Osaka, Biomater 23 (2002) 1353.
[11] M. Wieland, M. Textor, N.D. Spencer, D.M. Brunette, Int. J. Oral Maxillofac. Implants 16 (2) (2001) 163.
[12] P. Li, I. Kangasniemi, K.D. Groot, T. Kokubo, J. Am. Ceram. Soc. 77 (1994) 2307.
[13] N. Huang, P. Yang, X. Cheng, Y. Leng, X. Zheng, G. Gai, Z. Zhen, F. Zhang, Y. Chen, X. Liu, T. Xi, Biomater 19 (1998) 771.
[14] Y.T. Sul, C.B. Johansson, Y. Jeong, A. Wennerberg, T. Albrektsson, Clin. Oral. Implants Res. 13 (2002) 252.
[15] B. Feng, J.Y. Chen, S.K. Qi, L. He, J.Z. Zhao, X.D. Zhang, J. Mater. Sci Mater. Med. 13 (2002) 457.
[16] J. Yang, S. Mei, J.F.M. Ferreira, Scr. Mater. 46 (2002) 101.
[17] K.L. Ou, Microelectron. Eng. 83 (2) (2006) 312.
[18] P.H. Krogh, P. Worthington, W.H. Davis, E.E. Keller, Int. J. Oral Maxillofac. Implants 9 (2) (1994) 249.
[19] Y.C. Shyng, H. Devlin, K.L. Ou, Int. J. Prosthodont. 19 (2006) 513.
[20] M.C. Sunny, C.P. Sharma, J. Biomater. Appl. 6 (1991) 89.
[21] K. Yamanouchi, N. Sakurai, T. Satoh, Proc. IEEE Ultrason. Symp. (1989) 351.
[22] B.D. Ratner, J. Biomed. Mater. Res. 27 (1993) 837.
[23] T.R. Katona, N.H. Paydar, H.U. Akay, J. Biomech. 28 (1995) 27.
[24] W.E. Roberts, R.K. Smith, Y. Zilberman, Am. J. Orthod. 86 (1984) 95.
[25] W.E. Roberts, J. Dent. Educ. 52 (1988) 804.